

# Flexible Calibration of a Portable Structured Light System through Surface Plane

GAO Wei<sup>1</sup>    WANG Liang<sup>1</sup>    HU Zhan-Yi<sup>1</sup>

**Abstract** For a portable structured light system, it must be easy to use and flexible. So the inconvenient and expensive equipment for calibration such as two or three orthogonal planes or extra fixed equipment should not be considered. For the purpose of fast 3D acquisition, the projection matrices of a portable structured light system should be estimated. This paper proposes a flexible calibration method to meet the requirements of the portable structured light system through a surface plane. A calibration board is attached to the surface plane, and a reference pattern is also projected by an LCD projector onto the surface plane. The camera observes the surface plane at a few different positions. Then, the world-to-image point pairs for the camera and projector are obtained based on the cross ratio and epipolar geometry, and the system is thus calibrated. The experiments conducted for the proposed calibration method demonstrate its accuracy and robustness.

**Key words** Projector calibration, camera calibration, portable structured light system

Research on shape reconstruction and object recognition by projecting structured light stripes onto objects has been active since the early 1970s. Due to their fast speed and non-contact nature, structured light techniques have found numerous applications. A basic structured light system consists of a camera and a light (or laser) stripe projector, in which the projector projects light stripes on a measured object and the camera obtains images of the light stripes modulated by the depth of the object. Unlike a classic stereo vision system, the structured light system can generate dense world points by sampling image points on each light stripe in the image and alleviate the so-called correspondence problem.

Although the difficult matching problem can be alleviated, the structured light system must be fully calibrated before measuring an object<sup>[1]</sup>. The existing approaches to calibrate a structured light system take two steps: camera calibration and projector calibration. The camera calibration has been well studied. The world-to-image perspective matrix and the distorted coefficients are estimated using at least 6 noncoplanar world points and their corresponding projected image points. For the projector calibration, two main approaches are proposed. One is to estimate the coefficients of the equation of each light stripe plane relative to the same world system. For each light stripe plane, at least 3 noncollinear world points that fall onto the light stripe plane are required<sup>[2-4]</sup>. The other is to view the projector as an inverse camera, and a set of world-to-image point pairs (at least 6) is used to estimate the perspective matrix of the projector<sup>[5-7]</sup>.

For a portable structured light system, it must be easy to use and be flexible. So the inconvenient and expensive equipment for calibration such as two or three orthogonal planes<sup>[2-3, 5]</sup> or extra fixed equipment<sup>[6-8]</sup> should not be considered. The calibration method to estimate each light stripe plane<sup>[2-4]</sup> will give much computation burden when many stripes that are not suited for rapid 3D acquisition are projected. Different from the above methods, a flexible calibration method is proposed for the portable structured light system in this paper. Our method uses a calibration board, which is a paper sheet with circular control

points printed on a laser printer. It is attached to a surface plane and a reference pattern, which is an electronically designed pattern with some horizontal red stripes and one green stripe and projected onto the surface plane by an LCD projector. The surface plane is observed by the camera at a few different positions. Based on the cross ratio and the epipolar geometry, the world-to-image point pairs for the projector and camera are obtained, and the system is conveniently calibrated.

The rest of the paper is organized as follows. Section 1 presents some preliminaries. The proposed flexible calibration method is detailed in Section 2. Section 3 reports some experiments and some conclusions are listed in Section 4.

## 1 Preliminaries

Throughout the paper, we denote the known world points by upper case  $\mathbf{M}$  with the superscript  $w$ , e.g.  $\mathbf{M}^w = [x^w, y^w, z^w]^T$ , and denote the image points by lower case  $\mathbf{m}$  with the superscript  $c$  for the image points of the camera and the superscript  $p$  for the image points of the projector, e.g.  $\mathbf{m}^c = [u^c, v^c]^T$  and  $\mathbf{m}^p = [u^p, v^p]^T$ . Homogeneous coordinates are denoted by adding a “ $\sim$ ” above the entities, e.g.  $\widetilde{\mathbf{M}}^w = [x^w, y^w, z^w, 1]^T$ .  $o^c x^c y^c z^c$  is the camera system.  $o^w x^w y^w z^w$  is the world system with its  $x^w y^w$  axes on the calibration surface plane, to which the calibration board is attached, and  $z^w$  axis perpendicular to the surface plane and pointing toward the structured light system.

### 1.1 Camera and projector model

The camera used here is of the pinhole model. Under the model, a 3D point  $\mathbf{M}^w$  is projected to an image point  $\mathbf{m}^c$  by

$$\widetilde{\mathbf{m}}^c \propto K^c [R^c \mathbf{t}^c] \widetilde{\mathbf{M}}^w \quad (1)$$

where “ $\propto$ ” stands for the equality up to a scale factor;  $[R^c \mathbf{t}^c]$ , called the extrinsic parameters matrix, represents the rotation and translation between the world system and the camera system; and  $K^c$  is the camera's intrinsic parameters matrix of the form

$$K^c = \begin{bmatrix} \alpha & \gamma & u_0 \\ 0 & \beta & v_0 \\ 0 & 0 & 1 \end{bmatrix}$$

where  $(u_0, v_0)$  are the coordinates of the principle point,  $\alpha$  and  $\beta$  the focal lengths along the  $u$  and  $v$  axes of the image plane, and  $\gamma$  the parameter describing the skewness of the two image axes.

Received August 13, 2007; in revised form February 19, 2008  
Supported by National Key Technology Research and Development Program of China (2006BAK31B04) and National High Technology Research and Development Program of China (863 Program) (2007AA01Z341)

1. National Laboratory of Pattern Recognition, Institute of Automation, Chinese Academy of Sciences, Beijing 100190, P. R. China  
DOI: 10.3724/SP.J.1004.2008.01358

For the camera lens distortion, we use the following model. Let  $(x_u, y_u)$  be the ideal (undistorted) image coordinates, and  $(x_d, y_d)$  the corresponding real observed (distorted) image coordinates; then,

$$x_d = x_u + x_u r^2 (k_1 + k_2 r^2) + 2k_3 x_u y_u + k_4 (r^2 + 2x_u^2) \quad (2)$$

$$y_d = y_u + y_u r^2 (k_1 + k_2 r^2) + k_3 (r^2 + 2y_u^2) + 2k_4 x_u y_u \quad (3)$$

where  $r^2 = x_u^2 + y_u^2$ ,  $k_1$  and  $k_2$  are the coefficients of the radial distortion,  $k_3$  and  $k_4$  are the coefficients of the tangential distortion.

The model for the projector is the same as the one for the camera without lens distortion. So the relationship between a 3D point  $\mathbf{M}^w$  and its image projection  $\mathbf{m}^p$  can also be expressed as

$$\tilde{\mathbf{m}}^p \propto K^p [R^p \mathbf{t}^p] \tilde{\mathbf{M}}^w \quad (4)$$

where  $[R^p \mathbf{t}^p]$  represents the rotation and translation between the world system and the projector system, and  $K^p$  is the projector's intrinsic parameters matrix.

### 1.2 Cross ratio

Collinearity and cross ratio are known to be invariant under perspective projection. So, when the cross ratio  $r$  of collinear image points  $\mathbf{p}^c, \mathbf{q}^c, \mathbf{r}^c, \mathbf{m}^c$  and their three corresponding world points  $\mathbf{P}^w, \mathbf{Q}^w, \mathbf{R}^w$  are known, the coordinates of the fourth world point  $\mathbf{M}^w$  can be determined by the cross ratio.

### 1.3 Epipolar geometry

The epipolar geometry is the intrinsic projective geometry between two views<sup>[9]</sup>. It is independent of scene structure and only depends on the cameras' intrinsic parameters and relative pose. The fundamental matrix  $F$  encapsulates this intrinsic geometry. If a world point  $\mathbf{M}^w$  is projected to an image point  $\mathbf{m}^c$  in the first view, and  $\mathbf{m}'^c$  in the second, then, the image points satisfy

$$\tilde{\mathbf{m}}'^{cT} F \tilde{\mathbf{m}}^c = 0 \quad (5)$$

Given an image point  $\mathbf{m}^c$  in the first image, we can obtain a line  $\mathbf{l} = F\tilde{\mathbf{m}}^c$  in the second image. The corresponding point  $\mathbf{m}'^c$  in the second image must be lying on line  $\mathbf{l}$ . Line  $\mathbf{l}$  is called the epipolar line corresponding to  $\mathbf{m}^c$ .

## 2 A flexible calibration method

### 2.1 Camera calibration

Our calibration board is a paper sheet with circular control points. It is attached to a surface plane. The surface plane shown at a few different positions is taken by the camera. Then, the centroids of the circular control points at each position are detected. Using Zhang's method<sup>[10]</sup> and iterative refinement algorithms, the camera's intrinsic and extrinsic parameters including distortion coefficients are calibrated.

This part is rather conventional. The core of our system calibration is to calibrate the projector, where the key step is to make the projector able to see the surface plane, in other words, to indirectly derive the point correspondences from the surface plane to the projector's image (i.e. world-to-image point pairs). In the following section, this will be elaborated.

### 2.2 Fundamental matrix determination between the camera and the projector

To determine the fundamental matrix between the camera and the projector, a fundamental pattern is projected onto the surface plane by an LCD projector and captured by the camera. The fundamental pattern is an electronically designed grid composed of two green and some red lines, as shown in Fig. 1.

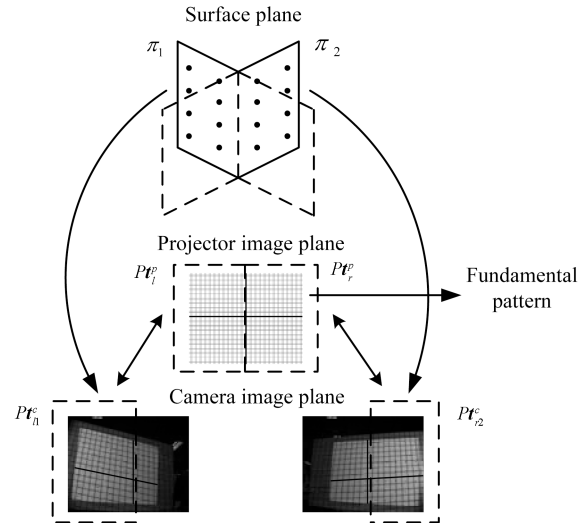


Fig. 1 Estimation of the fundamental matrix between the camera and the projector (Here, the bold lines denote the green lines and the grey lines denote the red lines. The meanings of the bold lines and grey lines in Figs. 2 ~ 5 are the same as those in Fig. 1.)

The two orthogonal green lines are to define the absolute positions of the intersection points. Then, the projected intersection points of lines on the projector image plane (i.e. fundamental pattern) and their corresponding images on the camera image plane are used to estimate the fundamental matrix. Since the normalized 8-points algorithm needs at least 8 noncoplanar points to compute the fundamental matrix, the surface plane is moved to another position and the second image is captured. The new position should be noncoplanar with the first one. Here, in Fig. 1, a pure rotation position is illustrated. The intersection points on the left side of the vertical green line in the fundamental pattern are denoted by  $Pt_i^p$  and those on the right side are denoted by  $Pt_r^p$ . The corresponding points to  $Pt_i^p$  on the first image are denoted by  $Pt_i^c$  and those to  $Pt_r^p$  on the second image are denoted by  $Pt_r^c$ . Then, the two sets of the corresponding point pairs  $(Pt_i^p, Pt_i^c)$  and  $(Pt_r^p, Pt_r^c)$  are noncoplanar and can be used to estimate the fundamental matrix  $F$ .

### 2.3 Determining the world-to-image point pairs for the projector

Although the projector is always viewed as an inverse camera, it can not capture the real image of the objects. So given the image points of the projector, its corresponding world position can not be decided directly. For determining the world-to-image point pairs for the projector, a reference pattern is projected onto the surface plane. The reference pattern is composed of one green and some red horizontal lines, as shown in Fig. 2.

The green line is to define the absolute positions of the

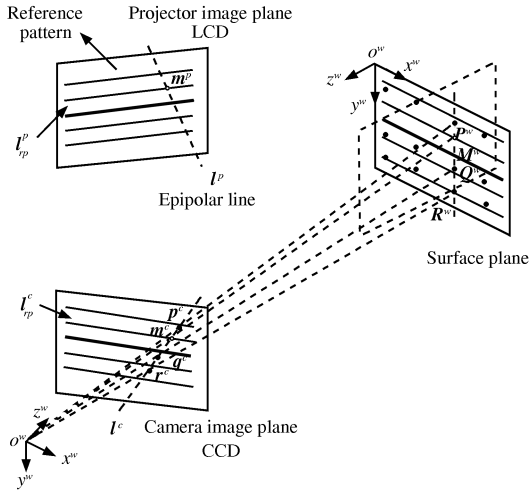


Fig. 2 Computation of the world-to-image point pairs for the projector

red lines. The centroids of the circular control points are detected. For each set of vertical collinear circular points, their images can be used to fit a line and  $l^c$  denotes one of fitted lines, as shown in Fig. 2. The image of the projection of the reference pattern is composed of many lines and  $l_{rp}^c$  denotes one of such lines. The point  $m^c$  is the intersection point between the fitted line  $l^c$  and line  $l_{rp}^c$ . Given three images of circular points  $p^c$ ,  $q^c$ , and  $r^c$  on line  $l^c$ , their corresponding world points  $P^w$ ,  $Q^w$ , and  $R^w$  on the calibration board are known. Since  $m^c$  is collinear with  $p^c$ ,  $q^c$ , and  $r^c$ , a cross ratio can be computed. A simple parameterization is given as

$$(q - p)\theta + p \quad (6)$$

where  $\theta$  is the parameter that defines points on the line. The cross ratio  $r$  of the four image collinear points is then defined as

$$r = \frac{\left( \frac{\theta_{p^c} - \theta_{r^c}}{\theta_{q^c} - \theta_{r^c}} \right)}{\left( \frac{\theta_{p^c} - \theta_{m^c}}{\theta_{q^c} - \theta_{m^c}} \right)} \quad (7)$$

Then, the world point  $M^w$  on the surface plane corresponding to the camera image point  $m^c$  can be determined by

$$\theta M^w = \frac{r(\theta_{Q^w} - \theta_{R^w})\theta_{P^w} - \theta_{Q^w}(\theta_{P^w} - \theta_{R^w})}{r(\theta_{Q^w} - \theta_{R^w}) - (\theta_{P^w} - \theta_{R^w})} \quad (8)$$

For line  $l_{rp}^c$  on the camera image plane, the corresponding line  $l_{rp}^p$  on the reference pattern can be decided by the green line. Given the camera image point  $m^c$  on line  $l_{cp}^c$ , an epipolar line  $l^p$  can be obtained by  $l^p = F\tilde{m}^c$ . The projector image point  $m^p$  corresponding to  $m^c$  must lie on  $l^p$ . Since  $m^p$  also lies on  $l_{rp}^p$ ,  $m^p$  can be obtained by  $\tilde{m}^p = l^p \times l_{rp}^p$ . So, the world-to-image point pair  $(M^w, m^p)$  for the projector is computed. Note that the  $x^w y^w$ -plane of the world system coincides with the surface plane, then, a world point  $M^w$  on the surface plane becomes  $M^w = [x^w, y^w, 0]^T$ .

## 2.4 Projector calibration

Once a number of world-to-image point pairs  $(M^w, m^p)$  for the projector are obtained as described above, and using Zhang's method once again, the projector's intrinsic and extrinsic parameters can be calibrated.

## 2.5 System calibration

In the above calibration procedure, we attach the world system to the surface plane. For calibrating the extrinsic parameters of the system, a unique world system for the camera and the projector has to be established. Without loss of generality, the world system can be attached to the camera system, then,

$$M^c = [I \ 0] \tilde{M}^w \quad (9)$$

$$M^p = [R \ t] \tilde{M}^w \quad (10)$$

where  $[R, t] = [R^p(R^c)^{-1}, -R^p(R^c)^{-1}t^c + t^p]$ ,  $M^c = [x^c, y^c, z^c]^T$ , and  $M^p = [x^p, y^p, z^p]^T$  are the coordinates of a 3D point  $M^w$  in the camera and projector system, respectively. So, the structured light system is finally calibrated. Then, we can get the 3D coordinates of the object with the estimated calibration parameters.

## 2.6 Summary

In summary, the calibration procedure of the proposed method is as follows.

**Step 1.** Print the calibration board on a laser printer and attach it to a surface plane;

**Step 2.** Project the fundamental pattern onto the surface plane, and take 2 images (denoted by  $I_f$ ) of the surface plane under 2 different positions;

**Step 3.** Project the reference pattern onto the surface plane, and take a few images (denoted by  $I_r$ ) of the surface plane under different positions;

**Step 4.** Calibrate the camera with  $I_r$ , then, correct  $I_f$  and  $I_r$  with distortion coefficients to obtain undistorted images, denoted by  $I_{uf}$  and  $I_{ur}$ , respectively;

**Step 5.** Estimate the fundamental matrix between the camera and the projector with  $I_{uf}$ ;

**Step 6.** Determine the world-to-image point pairs for the projector with  $I_{ur}$ ;

**Step 7.** Calibrate the projector with the point pairs in Step 6.

## 3 Experiments

The experiments for testing our proposed calibration method are reported here. The projector used in our system is 3M MP7740i, with a resolution set of  $1024 \times 768$  and the camera is Basler A101fc with a resolution set of  $1300 \times 1030$ . The working volume depends on the focusing capability and the field of camera's view. The object is usually placed at  $1000 \sim 1500$  mm from the system. The calibration board contains 70 circular control points ( $7 \times 10$ ). The distance between two points is 42.3 mm. 9 images of the surface plane under different positions are taken, as shown in Fig.3 (only 3 images illustrated). From these images, we can observe a significant lens distortion in the images.

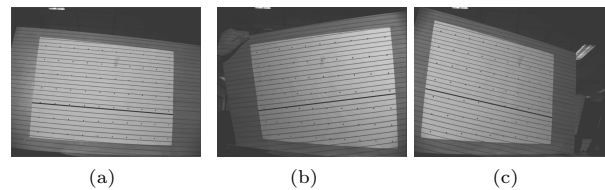


Fig. 3 Camera images of the surface plane at different positions

Table 1 shows the estimated calibration results of the camera and the projector. A residual error of reprojection

is measured to assess the estimated calibration matrix. The estimated transformation matrix  $[R \mathbf{t}]$  between the camera and the projector system is

$$[R \mathbf{t}] = \begin{bmatrix} 0.9992 & 0.0383 & 0.0124 & -23.1775 \\ -0.0271 & 0.8685 & -0.4950 & 139.2396 \\ -0.0297 & 0.4942 & 0.8688 & 330.4483 \end{bmatrix}$$

Table 1 The estimated camera and projector parameters

	$\alpha$	$\beta$	$\gamma$	$u_0$	$v_0$
Camera	1 865.82	1 852.33	-3.73	676.99	562.26
Projector	1 581.51	1 565.76	1.15	513.49	694.99
	$k_1$	$k_2$	$k_3$	$k_4$	Residual error
Camera	-0.3062	0.1211	0.0020	0.0054	0.6245
Projector	/	/	/	/	0.4282

Because the reference pattern has the green line to encode the different red lines, it can be applied to one-shot reconstruction. From the calibration images, the circular control points which lie on the light stripes are selected for reconstruction. From each image, 2 or 3 points are chosen. The true distance between the points and estimated value are computed, as shown in Table 2. The chosen points are denoted as  $(r, c)$  ( $r, c$  denote the row and column index, respectively). In Table 2, only the results at the first 5 positions are listed and the estimated accuracy of point distance at the other positions are consistent with those in Table 2 and are omitted due to the space limit. Because the camera used in this work has significant lens distortion, the reconstructed circular points at the periphery in the image are less accurate than those in the central region.

Table 2 The calibration accuracy evaluation with chosen control points

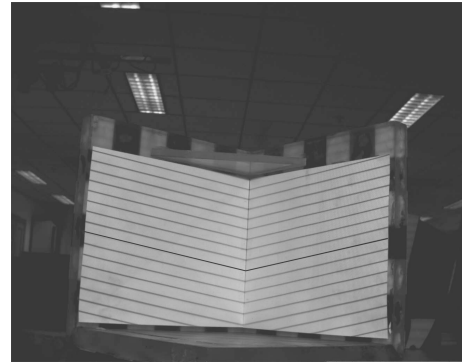
Number	True distance (mm)	Estimated value (mm)	Absolute error (mm)	Relative error (%)	
(1,8)(3,1)	307.9486	308.2486	0.3000	0.10	
Position 1	(3,1)(6,1)	126.9000	126.3976	0.5024	0.40
	(1,8)(6,1)	363.8784	364.7496	0.8712	0.24
Position 2	(3,6)(4,9)	133.7643	133.5370	0.2273	0.17
	(4,9)(5,6)	133.7643	133.5906	0.1737	0.13
	(3,6)(5,6)	84.6000	84.7852	0.1852	0.22
Position 3	(1,3)(1,4)	42.3000	42.3672	0.0672	0.16
	(1,4)(6,10)	330.3736	328.9544	1.4192	0.43
Position 4	(1,3)(6,10)	363.8784	362.2514	1.6270	0.45
	(1,8)(2,10)	94.5857	94.2269	0.3588	0.38
Position 5	(4,2)(4,9)	296.1000	295.6529	0.4471	0.15
	(4,9)(7,4)	246.6493	247.0369	0.3876	0.16
	(4,2)(7,4)	152.5148	152.0014	0.5134	0.34

Finally, we reconstruct an object which consists of two perpendicular surfaces, as shown in Fig. 4. At each surface, we fit the measured points with a flat plane and calculate the distances from the measured points to the fitted plane. The angle between the two estimated flat planes is also computed. The result is shown in Table 3. We also use the system to model a plaster statue. Fig. 5 shows the captured image and reconstructed results with texture mapping at

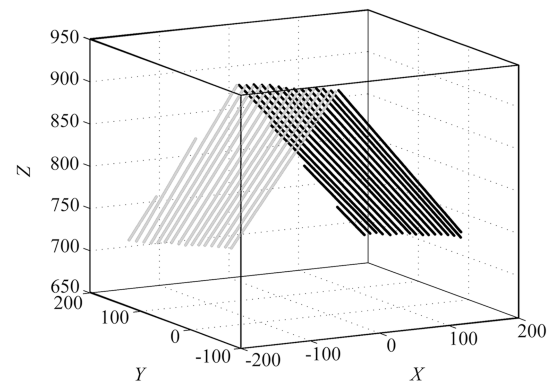
different view directions.

Table 3 The mean, standard deviation of distances and the angle between two estimated flat planes

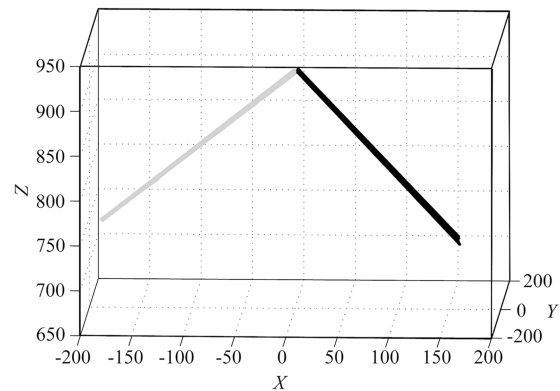
Distance to $\pi_1$ (mm)		Distance to $\pi_2$ (mm)		Angle ( $^\circ$ )
Mean	Std	Mean	Std	$(\pi_1, \pi_2)$
$-5.0 \times 10^{-4}$	0.5859	$-6.0 \times 10^{-4}$	0.5742	91.0085



(a) The original image of the two perpendicular surfaces



(b) The image under different view angles of the reconstructed surface

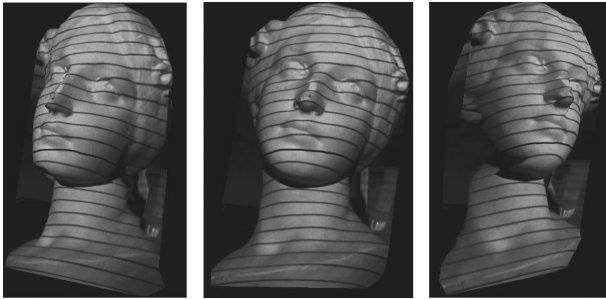


(c) The image under different view angles of the reconstructed surface

Fig. 4 Original image and reconstructed images



(a) The image of the statue taken by the camera



(b) ~ (d) The image under different view angles of the reconstructed statue

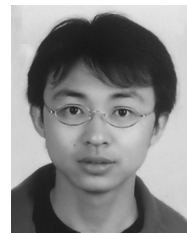
Fig. 5 A plaster statue reconstruction

## 4 Conclusions

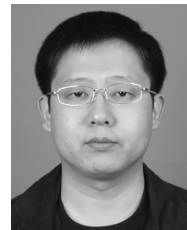
For a portable structured light system, it must be easy to use and be flexible. We present a flexible calibration method to calibrate the structured light system without using the inconvenient and expensive equipment such as two or three orthogonal planes or extra fixed equipment. Based on the cross ratio and epipolar geometry, the system can be calibrated through a surface plane. The experiments show that the proposed method is accurate and robust.

### References

- 1 Jarvis R A. A perspective on range finding techniques for computer vision. *IEEE Transactions on Pattern Analysis and Machine Intelligence*, 1983, **5**(2): 122–139
- 2 Wang G H, Hu Z Y, Wu F C, Tsui H T. Implementation and experimental study on fast object modeling based on multiple structured stripes. *Optics and Lasers in Engineering*, 2004, **42**(6): 627–638
- 3 Huynh D Q, Owens R A, Hartmann P E. Calibrating a structured light stripe system: a novel approach. *International Journal of Computer Vision*, 1999, **33**(1): 73–86
- 4 Zhou F Q, Zhang G J. Complete calibration of a structured light stripe vision sensor through planar target of unknown orientations. *Image and Vision Computing*, 2005, **23**(1): 59–67
- 5 Shin D, Kim J. Point to point calibration method of structured light for facial data reconstruction. *Lecture Notes in Computer Science*, 2004, **3072**: 200–206
- 6 Li J L, Hassebrook L G. Robust svd-based calibration of active range sensors. In: *Proceedings of SPIE Conference on Visual Information Processing*. Orlando, USA: SPIE, 2000. 68–77
- 7 Zhang S, Huang P S. Novel method for structured light system calibration. *Optical Engineering*, 2006, **45**(8): 1–8
- 8 Legarda-Saenz R, Bothe T, Juptner W P. Accurate procedure for the calibration of a structured light system. *Optical Engineering*, 2004, **43**(2): 464–471
- 9 Hartley R, Zisserman A. *Multiple View Geometry in Computer Vision*. Cambridge: Cambridge University Press, 2000
- 10 Zhang Z Y. A flexible new technique for camera calibration. *IEEE Transactions on Pattern Analysis and Machine Intelligence*, 2000, **22**(11): 1330–1334



**GAO Wei** Ph.D. candidate at the Institute of Automation, Chinese Academy of Sciences. His research interest covers image processing, 3D reconstruction, and augmented reality. Corresponding author of this paper. E-mail: wgao@nlpr.ia.ac.cn



**WANG Liang** Lecturer at Beijing University of Technology. He received his Ph.D. degree from the Institute of Automation, Chinese Academy of Sciences. His research interest covers camera calibration, 3D reconstruction, and mobile robot. E-mail: wangliang@bjut.edu.cn



**HU Zhan-Yi** Professor at the Institute of Automation, Chinese Academy of Sciences. He received his Ph.D. degree in computer science from University of Liege, Belgium, in 1993. His research interest covers camera calibration, 3D reconstruction, Hough transform, and vision guided robot navigation. E-mail: huzy@nlpr.ia.ac.cn